Folia Microbiologica (2018) 63:773–787
https://doi.org/10.1007/s12223-018-0619-y

ORIGINAL ARTICLE

Production and cleavage of a fusion protein of porcine trypsinogen and enhanced green fluorescent protein (EGFP) in *Pichia pastoris*

Hana Raschmanová[1,2] · Leona Paulová[1] · Barbora Branská[1] · Zdeněk Knejzlík[3] · Karel Melzoch[1] · Karin Kovar[2]

Received: 25 September 2017 / Accepted: 23 May 2018 / Published online: 5 June 2018

Abstract

Pharmaceutical grade trypsin is in ever-increasing demand for medical and industrial applications. Improving the efficiency of existing biotechnological manufacturing processes is therefore paramount. When produced biotechnologically, trypsinogen—the inactive precursor of trypsin—is advantageous, since active trypsin would impair cell viability. To study factors affecting cell physiology and the production of trypsinogen in fed-batch cultures, we built a fusion protein of porcine trypsinogen and enhanced green fluorescent protein (EGFP) in *Pichia pastoris*. The experiments were performed with two different pH values (5.0 and 5.9) and two constant specific growth rates (0.02 and 0.04 1/h), maintained using exponential addition of methanol. All the productivity data presented rely on an active determination of trypsin obtained by proteolysis of the trypsinogen produced. The pH of the medium did not affect cell growth, but significantly influenced specific production of trypsinogen: A 1.7-fold higher concentration of trypsinogen was achieved at pH 5.9 (64 mg/L at 0.02 1/h) compared to pH 5.0. EGFP was primarily used to facilitate detection of intracellular protein over the biosynthetic time course. Using flow cytometry with fluorescence detection, cell disruption was avoided, and protein extraction and purification prior to analysis were unnecessary. However, Western blot and SDS-PAGE showed that cleavage of EGFP-trypsinogen fusion protein occurred, probably caused by *Pichia*-endogenous proteases. The fluorescence analysis did therefore not accurately represent the actual trypsinogen concentration. However, we gained new experimentally-relevant insights, which can be used to avoid misinterpretation of tracking and quantifying as well as online-monitoring of proteins with the frequently used fluorescent tags.

Abbreviations

AOX1	Alcohol oxidase 1
CDW	Cell dry weight
EGFP	Enhanced greed fluorescent protein

Introduction

Trypsin, a serine endopeptidase catalyzing the cleavage of peptide bonds, is in ever-increasing demand for medical and industrial applications. Though built in the vertebrate pancreas (Walsh et al. 1964), extraction of trypsin from animal and human tissues as a possible manufacturing method is neither completely ethically acceptable nor safe. One of its major applications is the use of trypsin for the production of insulin. Insulin precursors are manufactured in biotechnological processes and then converted into insulin using proteolysis by trypsin or a combination of trypsin and carboxypeptidase B. As the number of people with diabetes is expected to rise to 522 million by 2030 (from 366 million diabetics in 2011)

✉ Hana Raschmanová
hana.raschmanova@vscht.cz

Leona Paulová
leona.paulova@vscht.cz

Barbora Branská
barbora.branska@vscht.cz

Zdeněk Knejzlík
zdenek.knejzlik@vscht.cz

Karel Melzoch
karel.melzoch@vscht.cz

Karin Kovar
karin.kovar@zhaw.ch

[1] Department of Biotechnology, University of Chemistry and Technology Prague, Technická 5, 166 28 Prague 6, Czech Republic

[2] Institute of Chemistry and Biotechnology, Zurich University of Applied Sciences (ZHAW), Grüentalstrasse 14, 8820 Wädenswil, Switzerland

[3] Department of Biochemistry and Microbiology, University of Chemistry and Technology Prague, Technická 5, 166 28 Prague, Czech Republic

(Whiting et al. 2011), the demand for good quality insulin at an affordable price is increasing, and thus also for trypsin.

For the production of trypsin/trypsinogen of any animal origin in a microbial host organism, recombinant technology provides the desired safe and scalable manufacturing alternative to tissue extraction. Ideally, the recombinant enzyme would be secreted and harvested from the culture/biomass supernatant. The methylotrophic yeast *Pichia pastoris* (reclassified as *Komagataella pastoris* (Yamada et al. 1994, 1995)) is one of the most widely studied yeasts, and a popular and established host system for the production of secreted recombinant proteins (Ahmad et al. 2014; Looser et al. 2015; Yang and Zhang 2017; Zahrl et al. 2017; Juturu and Wu 2018). Generally, if produced by a microbial system, trypsinogen—the inactive precursor form of trypsin—is preferred, since trypsin as a free protease would impair the viability of the host cells (Hyka et al. 2010). Production of trypsin or trypsinogen of various origins with *P. pastoris* has been described (Hanquier et al. 2003; Hohenblum et al. 2003; Macouzet et al. 2005; Guerrero-Olazaran et al. 2009; Hyka et al. 2010; Ling et al. 2012, 2014; Paulova et al. 2012; Viader-Salvado et al. 2013; Shu et al. 2015; Zhang et al. 2018).

Auto-proteolytic activation of trypsinogen to trypsin, which is known to occur at high pH (Kunitz and Northrop 1934; Shu et al. 2015), should be avoided by appropriate process conditions, in particular, by low pH (Hanquier et al. 2003; Hyka et al. 2010), or alternatively by mutating the trypsinogen cleavage site (Hanquier et al. 2003). *P. pastoris* tolerates a fairly wide range of pH values (from 3.0 to 7.0). Thus, it would be appropriate to efficiently produce trypsinogen, which should remain stable in the culture supernatant at an acidic pH. On the other hand, it has been demonstrated that exposure to low pH in combination with overproduction of a heterologous (recombinant) protein can cause serious cell damage (Hyka et al. 2010). Thus, the requirements for optimum culture conditions to produce trypsinogen represent a compromise between these two contradictory requirements, which need to be further investigated.

Our research follows up an industrial Czech-Swiss Eureka project (with the participation of Lonza AG and Lonza Biotec s.r.o.), which focused on the development of a large-scale manufacturing process for a *P. pastoris* strain producing recombinant porcine trypsinogen. The results of this project, however, indicated that trypsinogen might accumulate in the cells under certain cultivation conditions. To investigate this hypothesis, we fused trypsinogen and EGFP (enhanced green fluorescence protein) as a suitable model to understand the dynamics of production of trypsinogen/trypsin in *Pichia pastoris* as well as to investigate both its possible secretion and intracellular retention (Fig. 1a). The nucleotide sequence coding for EGFP-trypsinogen was cloned under the control of the methanol inducible alcohol oxidase (*AOX1*) promoter. Fluorescence markers (tags) added to proteins are generally useful for quantifying protein levels as (a) they can be used to monitor the distribution and dynamics of a protein of interest in inaccessible intracellular environments (Snapp 2005) without cell disruption, extraction, and purification, and (b) they facilitate indirect online monitoring of the target protein as easily measured fluorescence (Snapp 2005; Broger et al. 2009; Sjöblom et al. 2012). In addition, flow cytometry was used to assess viability at the single-cell level after staining with propidium iodide, which penetrates impaired cell membranes.

Monitoring the fluorescence using a flow cytometer, we aimed to analyze not only the typically determined extracellular protein concentration of the secreted product in the culture medium, but also its possible intracellular accumulation and the physiological state of the cells (i.e., their viability), thus fully evaluating the effect of the chosen culture conditions on the productivity and viability. However, a certain cleavage of EGFP-trypsinogen fusion protein was observed, probably caused by *Pichia*-proteases. Since cleaved, the EGFP-fluorescence analysis did therefore not represent the actual trypsinogen concentration accurately. But, as EGFP could be produced only together with the protein (trypsinogen) fused, it was still a useful indicator of overall productivity. These observations presented may therefore bring new information about the cellular protease system and the kinetics of recombinant protein production, both currently underexplored phenomena in *P. pastoris*.

Material and methods

Strain construction

Construction of the expression plasmid pPICZ-α-A-GFP-Tryp

Chromosomal DNA from *P. pastoris* strain X-33, carrying the codon optimized sequence of *S. cerevisiae* mating α-factor fused with *P. pastoris*-codon-optimized gene of porcine trypsinogen, under the control of the *AOX1* promoter (Paulova et al. 2012), was isolated and used as a template for PCR amplification of the recombinant cassette. Primers against *AOX1* promoter and terminator were used (AOX5: GACTGGTT CCAATTGACAAGC and AOX3: GCAAATGGCATTCT GACATCC). The PCR product was cleaved by restriction endonucleases *Xho*I and *Xba*I and ligated into the same restriction sites in vector pPICZ-α-A (Invitrogen, Carlsbad, CA). The constructed plasmid pPICZ-α-A-Tryp was verified by sequencing. The EGFP sequence was amplified from plasmid pEGFP-C1 (Clontech, Mountain View, CA) by PCR using primers TCTCTCGAGAAAAGAGAGGCTGAAGC TGTGAGCAAGGGCGAGGAGCTGTTCACCGGGG (+XhoI-ste13-GFP) and GGAATTCCTTGTACAGCTCG TCCATGCCGAGAGTGATCC (-GFP-EcoRInonSTOP) and ligated to plasmid pPICZ-α-A-Tryp between *Xho*I and *Eco*RI

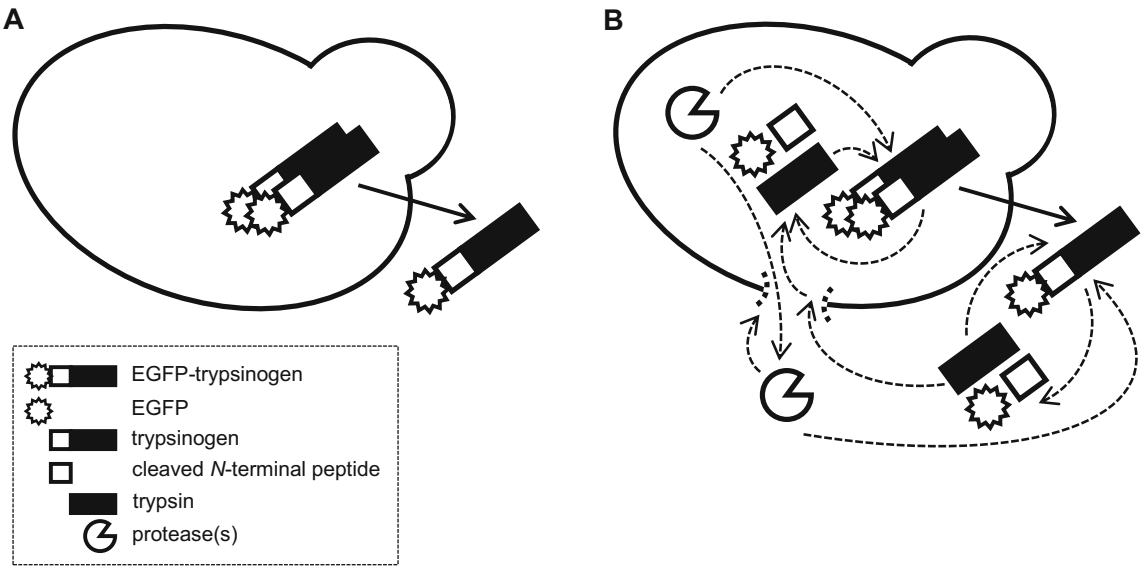

Fig. 1 Fusion protein of EGFP and trypsinogen produced by *Pichia pastoris*. The processes of production and secretion, and cleavage of the (recombinant) fusion protein are considered, and two hypothetical cases are depicted schematically: **a** The fusion protein is correctly synthesized and the intact protein is secreted from the cells, although a small proportion of the protein might be retained within the cells. The intracellular content of the fusion protein is detected using the EGFP-fluorescence signal. **b** Due to the combined action of activated trypsin and native intracellular protease(s), trypsinogen is activated to trypsin, and the fusion protein could be cleaved extra- or intracellularly. Autocatalytic activation of secreted trypsinogen to trypsin in the culture supernatant may occur, resulting in further activation of trypsinogen to trypsin, possibly impairing or even lysing the cells. The free trypsin might then enter cells through damaged cell membranes and further activate trypsinogen to trypsin and, in addition, cleave the fusion protein. Protease(s) present intracellularly might contribute to cleavage of the fusion protein as well as extracellularly, since they might be released from the cells through the damaged membranes

sites. The final expression plasmid (pPICZ-α-A-GFP-Tryp) was verified by DNA sequencing.

Transformation of *P. pastoris*

Plasmid pPICZ-α-A-GFP-Tryp was linearized by *Sac*I digestion in the *AOX1* promoter region and used for transformation of electrocompetent *P. pastoris* X-33 cells. Transformants were selected by Zeocin™ (Invitrogen, Carlsbad, CA) resistance of the transformation vector and tested for EGFP-trypsinogen production in minimal medium with methanol. The highest expressing clone was stored in 24% glycerol at − 80 °C and used for further studies.

Culture medium

Minimal methanol (MM) medium used for the selection of transformants contained 13.4 g yeast nitrogen base, 10 g methanol (≥ 99.8%, Penta), and 2 mL of filter sterilized biotin solution per liter.

The buffered complex medium with glycerol (BMGY) used for growth of the inoculum contained 10 g glycerol (≥ 99.5%, Penta), 10 g yeast extract, 20 g peptone, 100 mL 1 mol/L potassium phosphate buffer (pH 6.0), 100 mL filter sterilized YNB stock solution, 2 mL filter sterilized biotin stock solution, and 1 mL of 100 mg/mL Zeocin™ (Invitrogen, Carlsbad, CA) per liter. YNB solution, biotin solution, and Zeocin™ were added separately. The YNB stock solution contained 134 g/L yeast nitrogen base with ammonium sulfate and without amino acids. The biotin stock solution contained 0.20 g/L biotin.

Defined mineral medium used for batch bioreactor cultivations contained 30 g glycerol (≥ 99.5%, Penta) or 5 g methanol (≥ 99.8%, Penta) to calculate the growth parameters of the production strain on methanol as a sole carbon source, 0.17 g $CaSO_4$, 2.86 g K_2SO_4, 0.64 g KOH, 0.22 g NaCl, 2.32 g $MgSO_4 \cdot 7H_2O$, 0.6 g EDTA disodium dihydrate, 7.23 g H_3PO_4, 9.55 g NH_4Cl, 0.2 mL polypropylene glycol (PPG) per liter, 6.53 mL filter sterilized PTM1 solution, and 6.53 mL filter sterilized biotin solution per liter. The PTM1 stock solution contained 5.0 mL 96% H_2SO_4, 6.00 g $CuSO_4 \cdot 5H_2O$, 0.08 g NaI, 3.0 g $MnSO_4 \cdot H_2O$, 0.2 g $Na_2MoO_4 \cdot 2H_2O$, 0.02 g H_3BO_3, 0.92 g $CoCl_2 \cdot 6H_2O$, 20.0 g $ZnCl_2$, and 65.0 g $FeSO_4 \cdot 7H_2O$ per liter. Before inoculation, the pH of the medium was adjusted to 5.0 or 5.9 using 25% NH_4OH.

Concentrated medium used in the first phase of fed-batch (to support cell growth) contained 500 g glycerol (≥ 99.5%, Penta), 12 mL filter sterilized PTM1 solution, and 12 mL filter sterilized biotin solution per liter.

Concentrated medium used in the second phase of fed-batch (trypsinogen production) contained 500 g methanol (≥ 99.8%, Penta), 12 mL filter sterilized PTM1 solution, and 12 mL filter sterilized biotin solution per liter.

Inoculum growth

A glycerol stock (1 mL) of the strain was thawed and used to inoculate a shake flask with 150 mL of BMGY medium. This seed culture was grown for 24 h at 30 °C and 150 rpm, and then aseptically transferred to the bioreactor to achieve a 10% inoculation ratio.

Culture conditions

All batch cultivations with either glycerol (30 g/L) or methanol (5 g/L) as a sole carbon source were carried out in a 5-L bioreactor (BIOSTAT® B-DCU, B. Braun Biotech International, Germany), under the following conditions: temperature 30 °C, pH 5.0, working volume of 1.5 L, airflow of 1.5 L/min (1 VVM), and 800 rpm agitator speed. Ammonium hydroxide (25%) and sulfuric acid (10%) were used for pH adjustment.

The fed-batch always started after glycerol in batch (30 g/L) was completely consumed, which was indicated by a rapid increase in dissolved oxygen concentration in the medium (after approximately 20 h). The fed-batch consisted of two phases. Firstly, exponential feeding of glycerol solution was performed according to equation $F = 0.020 \cdot e^{0.2 \cdot t}$ (Eq. 3) to keep the specific growth rate with glycerol at a constant value of 0.2 1/h (i.e., close to the maximum specific growth rate of this strain with glycerol) to rapidly increase the biomass concentration. After 5 h of glycerol feeding, a methanol pulse (5 g/L) was performed as a "transition" phase prior to the initiation of methanol feeding, in order to avoid methanol accumulation during the shift in cellular metabolism. After methanol depletion (approx. 3 h), signaled by a steep increase in dissolved oxygen, the exponential addition of methanol solution to produce trypsinogen followed. The feeding of methanol $F = 0.010 \cdot e^{0.02 \cdot t}$ or $F = 0.020 \cdot e^{0.04 \cdot t}$ was calculated (Eq. 3) to keep the growth rate of cells at constant values of either 0.02 or 0.04 1/h (approximately 25 or 50% of μ_{max} on methanol, respectively). Exponential feeding of glycerol- or methanol-containing medium was performed using a programmable peristaltic pump (Watson Marlow 505S, Watson Marlow Limited, UK). The pH was maintained at either 5.0 or 5.9. Aeration during the methanol production phase was regulated by increasing the inlet airflow and/or agitation speed from 2.5 to 4.0 L/min and up to 1200 rpm, respectively, or by supplementation of the inlet gas with pure oxygen. Samples were withdrawn regularly during fed-batch culture.

Substrate analyses

Concentrations of glycerol and methanol were determined in culture supernatants by HPLC analysis (Agilent, Spain) using Polymer IEX H^+ column (Watrex Praha, Prague, Czech Republic) at 80 °C and a refractive index detector (Agilent, Santa Clara, CA). A mobile phase of 1 mmol/L H_2SO_4 in demineralized water was applied at a flow rate of 0.5 mL/min, with an injection volume of 20 μL.

Concentration of biomass

The concentration of biomass was determined gravimetrically as cell dry weight (CDW), the cells generally being collected from 1 mL samples, washed with distilled water and dried at 105 °C until constant mass.

Determination of trypsinogen concentration

Trypsinogen concentration in centrifuged supernatants (5000*g*, 5 min) was determined after activation with 1 mg/mL enterokinase (Sigma-Aldrich, St. Louis, USA) in 0.15 mol/L TEA buffer (pH 8.2) for 24 h at 4 °C. One unit of trypsin hydrolyzes 1 μmol of the chromogenic substrate, *N*-α-benzoyl-arginine-*p*-nitroanilide (BApNA), per minute at 25 °C and pH 8.2. Released *p*-nitroaniline was quantified at 405 nm with a Cary 50 Bio UV-Visible Spectrophotometer (Varian, Melbourne, Australia). The activity of trypsin in the supernatant was converted to a concentration (mg/L) using commercial trypsinogen (Sigma-Aldrich, St. Louis, USA) as a standard. The concentration of trypsinogen in the culture broth was calculated from the trypsinogen concentration in the supernatant, taking into account that the supernatant formed 75–80% of the working volume during the methanol fed-batch phase (because of the high concentration of biomass in the bioreactor).

Flow cytometric analysis

A flow cytometer (BD Accuri™ C6, BD Biosciences, Franklin Lakes, USA) equipped with a 20 mW 488 nm Solid State Blue Laser was employed for simultaneous measurement of intracellular EGFP (excitation/emission maxima of 488/507 nm), assessed as green fluorescence (FL1 530 ± 15 nm), and cell viability, assessed as integrity of the cytoplasmic membrane after staining the cells with propidium iodide (PI, excitation/emission maxima of 536/617 nm), analyzed as red fluorescence (FL3 670 ± 15 nm). PI effectively only enters cells with non-intact or damaged membranes and intercalates into double-stranded nucleic acids, resulting in a red fluorescence; such cells were considered as non-viable.

Prior to analysis, cells were centrifuged (2000*g*, 5 min), resuspended in filtered (0.22 μm, Sterifil™, Merck Millipore, Billerica, USA) phosphate-buffered saline (PBS) to an A_{600nm} of 0.5, and incubated with 10 μg/mL of PI for 5 min.

Protein analysis by SDS-PAGE and Western blot with immunochemical detection

Cell disintegration

The cell pellet obtained after centrifugation (5000*g*, 5 min) was resuspended in disintegration buffer (50 mmol/L sodium phosphate, pH 7.4, 1 mmol/L PMSF (phenylmethyl sulfonyl fluoride), 1 mmol/L EDTA, 5% glycerol), mixed with 425–600 μm glass beads (Sigma-Aldrich, St. Louis, USA) and 10% SDS, and disintegrated by vortexing in FastPrep®-24 (MP Biomedicals, Santa Ana, CA) at a maximum speed for 60 s, 4 cycles. The homogenate was centrifuged (20,000*g*, 10 min).

Protein separation and detection

The EGFP-trypsinogen fusion protein was analyzed in both the supernatant and cell homogenate by 12% Tris-tricine SDS-PAGE with Coomassie Blue staining, and Western blot with immunochemical detection (GFP Antibody, pAb, Rabbit, GenScript, Piscataway, USA as primary antibody in 1:1000 *v*/*v* dilution; goat anti-rabbit IgG-HRP, HRP conjugated, Santa Cruz Biotechnology, Dallas, USA, as secondary antibody in 1:4000 *v*/*v* dilution). The sample (cell homogenate, supernatant) was mixed with loading buffer (12.1 g Tris-HCl, 240 g glycerol, 0.2 g Coomassie Brilliant Blue R-250, 40 g SDS per liter) in a ratio of 1:2 *v*/*v* (cell homogenate) or 2:1 *v*/*v* (supernatant), boiled to denature protein secondary structure (100 °C, 5 min), and 15 μL of mixture was loaded onto the gel. For Coomassie Blue staining, a protein marker was loaded (6.500–200 kDa, SDS-PAGE Standards, Broad Range, Bio-Rad, Hercules, CA), and for Western blotting on a nitrocellulose membrane (0.45 μm, Bio-Rad, Hercules, CA), a pre-stained marker was used (ColorBurst™, Electrophoresis Marker, mol. wt 8000–220,000 Da, Sigma-Aldrich, St. Louis, USA). A chemiluminescence assay was performed to detect the immunochemical complex (SuperSignal™ West Femto Maximum Sensitivity Substrate, Thermo Scientific, Waltham, USA).

Data analysis

Maximum specific growth rate was calculated according to Eq. (1):

$$\mu_{\max} = \frac{\ln x(t) - \ln x_0}{t - t_0} \quad (1/\mathrm{h}) \tag{1}$$

where x is the biomass concentration (g/L) and t is the cultivation time (h).

Maximum biomass/substrate yield was calculated according to Eq. (2):

$$Y_{x/s,\ \max} = \frac{x_2 - x_1}{s_2 - s_1} \quad (\mathrm{g/g}) \tag{2}$$

where s is the substrate concentration (g/L).

Exponential feeding rate was calculated according to Eq. (3):

$$F = F_0 \cdot e^{\mu \cdot t} = \frac{\mu \cdot V_0 \cdot x_0}{Y_{x/s,\max} \cdot s_0} \cdot e^{\mu \cdot t} \quad (\mathrm{L/h}) \tag{3}$$

where F_0 is the initial feed rate (L/h), μ is the required specific growth rate (1/h), V_0 is the initial working volume (L), x_0 is the initial biomass concentration (g/L), and s_0 is the concentration of carbon source in the feed solution (g/L). The values are specified in Table 1.

Specific growth rate during fed-batch was calculated according to Eq. (4):

$$\mu(t) = \frac{\ln(x \cdot V) - \ln(x_0 \cdot V_0)}{t - t_0} \quad (1/\mathrm{h})\,. \tag{4}$$

Product/biomass yield during fed-batch was calculated according to Eq. (5):

$$Y_{p/x} = \frac{\Delta(c_p . V_S)}{\Delta(x . V)} \quad (\mathrm{mg/g}) \tag{5}$$

where c_p is the product concentration (mg/L).

Approximate volume of supernatant was calculated according to Eq. (6):

$$V_s(t) = \frac{(V(\mathrm{t}) \cdot \rho_{\mathrm{broth}}) - \frac{M_{x.\mathrm{WCW}}}{1000}}{\rho_{\mathrm{supernatant}}} \quad (\mathrm{L}) \tag{6}$$

where ρ_{broth} is the density of culture broth (kg/L), $M_{x,\ \mathrm{WCW}}$ is the mass of wet cells (g/L), and $\rho_{\mathrm{supernatant}}$ is the density of supernatant that is approximately 1.03 kg/L (Potgieter et al. 2010).

The density of culture broth was calculated according to Eq. (7):

$$\rho_{\mathrm{broth}} \approx 0.000132 \cdot x_{\mathrm{WCW}} + 1.03 \quad (\mathrm{kg/L}) \tag{7}$$

where x_{WCW} is the concentration of biomass wet cell weight (g/L).

The concentration of wet biomass (g/L) was calculated according to Eq. (8). This equation was determined and verified experimentally for the given strain and culture conditions.

$$\mathrm{WCW} \approx 4.2 \cdot \mathrm{CDW} \quad (\mathrm{g/L})\,. \tag{8}$$

Specific productivity was calculated according to Eq. (9):

$$q_p(\mu) = \mu . Y_{p/x} \quad (\mathrm{mg/g\ per\ h}) \tag{9}$$

Results

The maximum specific growth rates of the *P. pastoris* strain expressing EGFP-trypsinogen achievable with glycerol or

Table 1 Basic growth parameters of the *P. pastoris* strain growing on glycerol or methanol and expressing EGFP-porcine trypsinogen, and design of fed-batch cultivations. The basic growth parameters were calculated from the data obtained from batch cultivations (30 g/L glycerol or 5 g/L methanol)

Parameter	Glycerol	Methanol
	Calculated from batch cultivations	
μ_{max} (1/h)	0.210 ± 0.024	0.076 ± 0.005
$Y_{x/s,max}$ (g/g)	0.588 ± 0.004	0.279 ± 0.006
	Design of growth fed-batch	Design of production fed-batch
μ (1/h)	0.2	0.02 or 0.04
V_0 (L)	1.500	1.675
x_0 (g/L)	20	40
s_0 (g/L)	500	500
Duration (h)	5	24
F_0 (L/h)	0.020	0.010 or 0.020

methanol, together with the corresponding yields, were calculated from the batch cultivations (Table 1). These data, which lie within the interval of typical values for *P. pastoris* (Looser et al. 2015), were used to calculate exponential feeding rates of concentrated solutions of nutrients in fed-batch cultivations according to Eq. 3, to maintain the specific growth rate of cells at constant values (Table 1).

Effect of pH on cell growth, viability, and extracellular trypsinogen production

The effects of pH (5.0 or 5.9) on trypsinogen production, cell growth, and viability were studied during fed-batch cultivations with glycerol as a substrate in the growth phase (constant specific growth rate 0.2 1/h) and later methanol as a substrate in the production phase (constant specific growth rate 0.02 1/h) (Table 2, columns 1 and 2). As seen in Fig. 2 (top graph), growth of biomass with glycerol or methanol was almost identical at pH 5.0 and 5.9, and the same was true for cell viability, which was very high; less than 1% of the population was stained with propidium iodide (PI) during the cultivation process (data not shown). The intensity of intracellular green fluorescence emitted by EGFP rose shortly after the methanol pulse, indicating recombinant gene expression, and steadily increased during the fed-batch cultivation with methanol, as monitored by flow cytometry; the course of green fluorescence followed the same pattern at both pH values tested (Fig. 2, middle graph). In contrast, the pH of the medium significantly affected the extracellular concentration of trypsinogen (Fig. 2, bottom graph); by maintaining the pH at the higher value (5.9), a 1.7-fold higher extracellular concentration of trypsinogen was obtained over the production phase (methanol fed-batch) compared to the lower pH (5.0). The final extracellular concentration of trypsinogen was 64 mg/L

Table 2 Settings and values achieved in four fed-batch cultivations. Specific growth rates (μ) on glycerol and methanol were maintained by exponential feeding of the particular substrate. In cultivations (●), (○), and (□), the dissolved oxygen concentration was regulated only by increasing agitation speed and/or airflow rate, whereas in cultivation (■), pure oxygen was also added to the inlet gas. Specific growth rates achieved with glycerol or methanol, and specific productivities were calculated from the cultivation data

Cultivation	○	●	□	■
	Set values			
$\mu_{glycerol}$ (1/h)	0.2	0.2	0.2	0.2
$\mu_{methanol}$ (1/h)	0.02	0.02	0.04	0.04
pH	5.0	5.9	5.9	5.9
Oxygen supply	no	no	no	yes
	Reached values—glycerol fed-batch			
$\mu_{glycerol}$ (1/h)	0.229 ± 0.039	0.233 ± 0.044	0.203 ± 0.050	0.211 ± 0.029
	Reached values—methanol fed-batch			
Δt_1	0.0–8.8 h	0.0–5.5 h	0.0–11.2 h	0.0–9.3 h
Δt_2	8.8–21.2 h	5.5–21.2 h	11.2–21.6 h	9.3–21.1 h
$\mu_{methanol}$ (1/h) in Δt_1	0.020 ± 0.001	0.018 ± 0.001	0.035 ± 0.001	0.023 ± 0.002
$\mu_{methanol}$ (1/h) in Δt_2	0.020 ± 0.001	0.018 ± 0.001	0.035 ± 0.001	0.044 ± 0.003
q_p (mg/g/h) in Δt_1	0.032 ± 0.003	0.081 ± 0.016	0.028 ± 0.006	0.032 ± 0.008
q_p (mg/g/h) in Δt_2	0.010 ± 0.001	0.019 ± 0.003	0.000 ± 0.000	0.002 ± 0.000

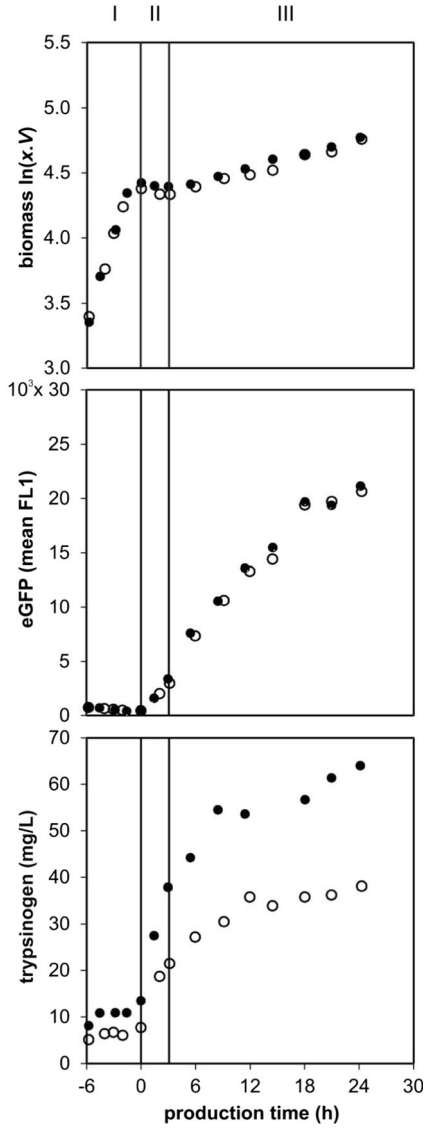

Fig. 2 Biomass growth and recombinant protein production at pH 5.9 or 5.0. Cultivation phases (as distinguished by the added substrate) are marked with roman numerals—(I) fed-batch with glycerol, (II) pulse of methanol, and (III) fed-batch with methanol. The specific growth rate with methanol was set at 0.02 1/h for all cultivations. Cultivation at pH 5.9 (filled circle) and cultivation at pH 5.0 (empty circle). Upper graph: biomass growth shown as the logarithm of total biomass (in grams) with time. Middle graph: the mean fluorescence of intracellular EGFP determined by flow cytometry and, thus, representing the sum of intracellular trypsinogen concentration and free EGFP; experimental distinction between these was not possible. Bottom graph: development of extracellular trypsinogen concentration with time

at pH 5.9, while at pH 5.0, it was only 38 mg/L (in total, 125 and 74 mg of trypsinogen were produced over the production phase, respectively). The specific extracellular productivity of trypsinogen followed a similar pattern in both cases; at pH 5.9, a high specific rate of trypsinogen production (0.081 ± 0.016) mg/g/h was maintained for the first 6 h of methanol fed-batch and then dropped to (0.019 ± 0.003) mg/g/h. In the case of a lower pH (5.0), the specific production rate (0.032 ± 0.003) mg/g/h decreased to (0.010 ± 0.001) mg/g/h after 9 h of growth with methanol fed exponentially (Table 2).

Effect of pH on the proteolytic cleavage of the fusion protein EGFP-trypsinogen

The fusion protein EGFP-trypsinogen was routinely detected by two methods: fluorescence of EGFP inside the cells was analyzed by flow cytometry, and the enzymatic activity of trypsinogen was evaluated only in the supernatant (i.e., extracellularly) by the enterokinase/BApNA assay. Therefore, an additional analysis was required that was readily applicable to both intracellular and extracellular contents of the fusion protein. Therefore, Western blot with α-GFP antibody was performed to specifically detect EGFP in the cells as well as in the medium. The immunochemical analysis brought unexpected results: Both inside the cells and in the medium, a cleaved EGFP with a molar mass of ca 27 kDa was detected. The EGFP content within cells was comparable in the samples taken at the same time points at pH 5.0 and 5.9 (Fig. 3a), which was in agreement with the flow cytometric analysis of EGFP fluorescence. However, the protein fragments containing EGFP detected with the α-GFP antibody in the cultivation medium were of a different character at pH 5.0 than at 5.9. While at the higher pH 5.9, only the cleaved EGFP (27 kDa) band was significant, at pH 5.0, the full-length EGFP-trypsinogen fusion protein (50 kDa), the cleaved EGFP (27 kDa), and another fragment of the fusion protein were detected (Fig. 3a).

Bands corresponding to EGFP (27 kDa) and trypsinogen (23 kDa) were observed in the samples of the cultivation medium after Coomassie Blue staining (Fig. 3b). The intensities of the EGFP and trypsinogen bands were always comparable within each sample, and the intensities were higher at pH 5.9, indicating a higher amount of the recombinant protein (though fragmented) in the cultivation medium at the higher pH. The higher pH promoted cleavage of the fusion protein EGFP, while at pH 5.0, the full-length fusion protein predominated.

In order to characterize the cleavage sites in the fusion protein, the fragments corresponding to EGFP and trypsinogen were analyzed by *N*-terminal sequencing. The first four amino acids in the *N*-terminal sequence of the cleaved EGFP fragment were EAEA, corresponding to the *C*-terminus of the α-leader sequence, followed by VSK, which are the first three amino acids at the EGFP *N*-terminus (Fig. 4). The *N*-terminus of the trypsinogen fragment began with YK, which are the two last amino acids of the EGFP sequence. This was followed by EFTDDD, which corresponds with the beginning of the trypsinogen sequence. This confirms that the EGFP fragment was the EGFP protein with the EAEA residue from the α-leader at its *N*-terminus, but without YK at its *C*-terminus. The trypsinogen fragment was trypsinogen with YK residues from EGFP at its *N*-terminus.

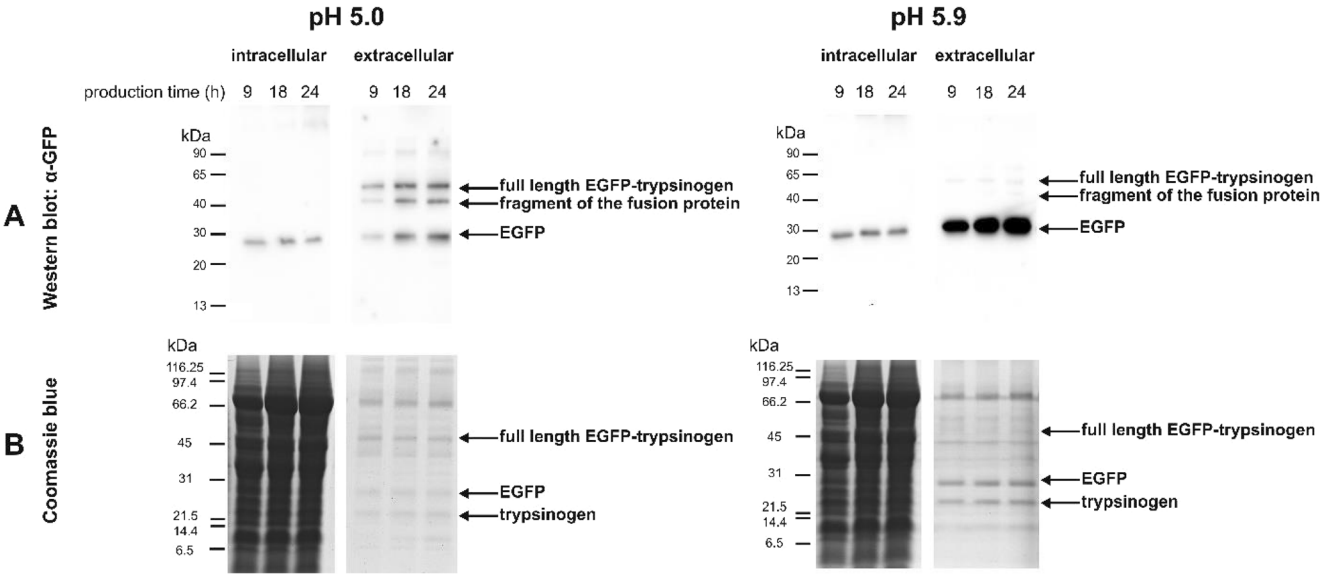

Fig. 3 Intracellular and extracellular recombinant protein from cultures grown at pH 5.9 or 5.0. The specific growth rate with methanol was set at 0.02 1/h in both cultivations. Recombinant product was analyzed at 9, 18, and 24 h after the methanol pulse by means of Western blot with immunochemical detection of EGFP (**a**) and Coomassie Blue staining (**b**). The volume of the sample loaded onto the gel was 5 μL for intracellular homogenate and 10 μL for the supernatant. SDS-PAGE was run in parallel, one gel stained with Coomassie Blue and the second one blotted on a nitrocellulose membrane. Specific α-GFP antibody was used for immunochemical detection of EGFP. The exposure time to obtain the chemiluminescence signal of the immunocomplex was 20 s. The protein bands of interest on the gel/membrane are the following: full-length fusion protein EGFP-trypsinogen (ca 50 kDa); cleaved EGFP (27 kDa); cleaved trypsinogen (23 kDa); and fragment of the fusion protein (not analyzed further)

Effect of methanol feeding rate on trypsinogen production, cell growth, and viability

Cell viability and trypsinogen production were studied in fed-batch culture using exponential feeding of methanol to maintain the specific growth rate at constant values of 0.02 1/h or 0.04 1/h (Table 2, columns 2 and 3); the growth phase with glycerol was the same as previously described. For both cultivations, the pH was kept at 5.9.

In the case of the lower methanol feed rate (0.02 1/h), all methanol fed into the bioreactor was immediately metabolized (Fig. 5, top graph) without accumulation in the culture broth; the specific growth rate of cells was close to that set by exponential feeding ((0.018 ± 0.001) 1/h), the biomass concentration steadily increased, reaching a final concentration of 61 g/L (i.e., ln(*x*.*V*) 4.8) (Fig. 6, top graph). As revealed by flow cytometry, cell viability was not affected over the production phase; only 1% of the cell population was stained with PI at the end of the process (Fig. 5, top graph).

When the higher methanol feed rate was applied to maintain a specific growth rate at 0.04 1/h (Table 2, column 3), the oxygen supply to the cells was not sufficient to satisfy the high demand for methanol metabolism and dissolved oxygen thus became a limiting factor shortly after the start of exponential feeding; this resulted in methanol accumulation (Fig. 5, top graph). As a consequence, the real specific growth rate with methanol was reduced to (0.035 ± 0.001) 1/h (Table 2, column 3), and the final biomass concentration was lower (62.4 g/L, i.e., ln(*x*.*V*) 5.0) than expected (Fig. 6, top graph). As seen in Fig. 5 (top graph), cells were able to cope with accumulated methanol until its concentration exceeded 10 g/L (after 15 h of exponential feeding), and then cell viability

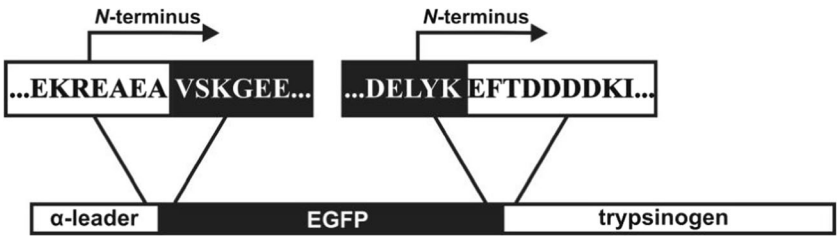

Fig. 4 Cleavage sites of the EGFP-trypsinogen fusion protein determined by *N*-terminal sequencing. The fragment obtained by SDS-PAGE, of size corresponding to EGFP (27 kDa), had EAEA amino acids in front of the EGFP. EAEA is at the end of an α-leader sequence, and VSK is at the *N*-terminal of EGFP. The *N*-terminal sequence of the fragment, whose mobility corresponded to trypsinogen (23 kDa), was YKEFTDDD. YK is the *C*-terminus of EGFP and EFTDDD is the *N*-terminal sequence of trypsinogen

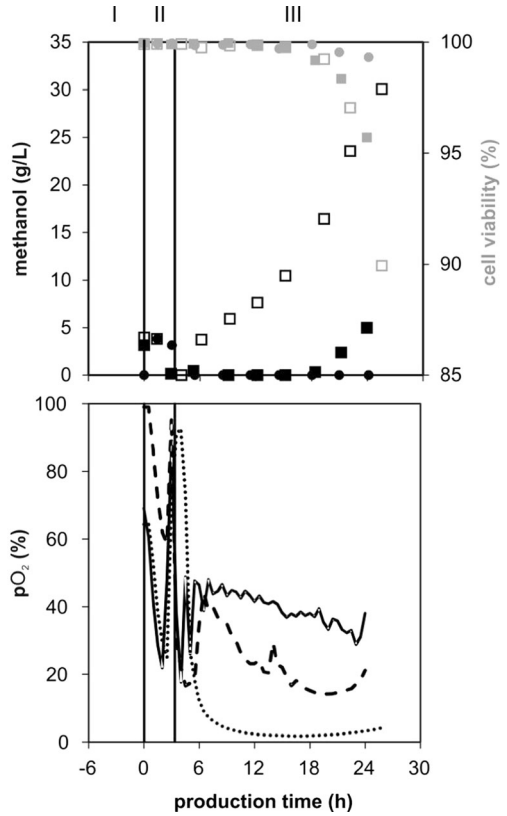

Fig. 5 Fed-batch cultivations with methanol performed at different specific growth rates and under different oxygen supplies. The pH of cultivation medium was 5.9 in all three cultivations. The cultivation phases are marked with roman numerals: (I) fed-batch with glycerol, (II) pulse of methanol, and (III) fed-batch with methanol, where the methanol accumulated to a different extent in the culture medium, possibly impairing cell viability. The filled circles (●) and full line represent cultivation at a specific growth rate with methanol set at 0.02 1/h and with no additional pure oxygen in the inlet air. The empty squares (□) and dotted line represent cultivation at a specific growth rate with methanol set at 0.04 1/h and with no additional pure oxygen in the inlet air. The filled squares (■) and dashed line represent cultivation at a specific growth rate with methanol set at 0.04 1/h and with inlet air supplemented with pure oxygen to maintain the dissolved oxygen concentration above 20% saturation. In the other two cultivations (filled circles and empty squares), there was no supplementation by oxygen and the aeration during the methanol production phase was regulated only by increasing the inlet airflow (from 2.5 to 4.0 L/min) and/or agitation speed (up to 1200 rpm). Upper graph: effects of different specific growth rates with methanol (cultivations, filled circles and empty squares) and the effect of oxygen availability (cultivations, empty squares and filled squares) on cell viability with methanol accumulated in the medium. The methanol concentration in the medium is represented by black symbols, and cell viability is represented by gray symbols. Cell viability was assessed as red fluorescence by flow cytometry after propidium iodide staining. Bottom graph: dissolved oxygen concentration in the cultivation medium during phases with methanol (II and III)

quickly declined. Intracellular EGFP content followed the same pattern as previously, until the methanol concentration in the bioreactor, after the methanol pulse, exceeded 3.8 g/L (Fig. 5, top graph); its intracellular content then rapidly increased, suggesting an accelerated synthesis of the recombinant protein

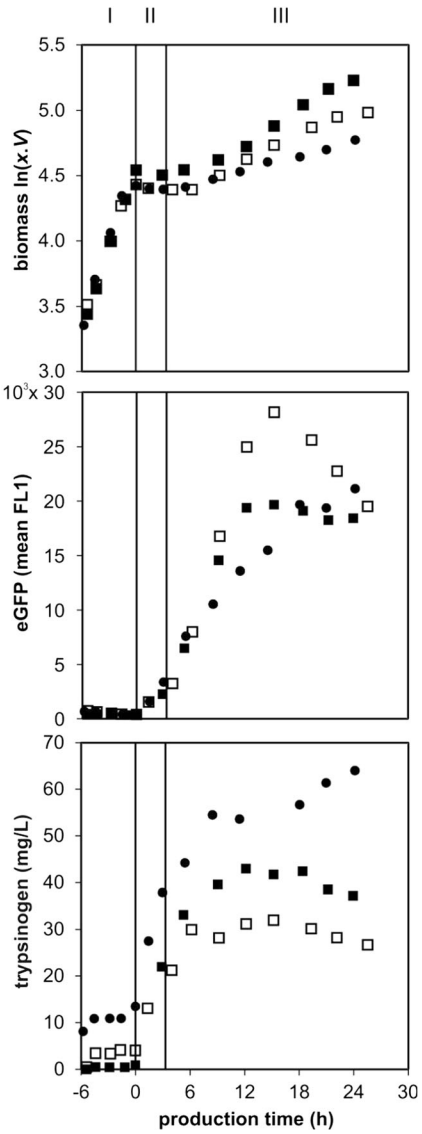

Fig. 6 Biomass growth and recombinant protein production as affected by different feeding rates of methanol (and correspondingly different specific growth rates) and different oxygen supplies. The pH of the cultivation medium was 5.9 in all three cultivations. The cultivation phases are marked with roman numerals—(I) glycerol fed-batch, (II) methanol pulse, and (III) methanol fed-batch. The filled circles (●) represent cultivation at a specific growth rate with methanol set at 0.02 1/h and with no additional pure oxygen in the inlet air, the empty squares (□) represent cultivation at a specific growth rate with methanol set at 0.04 1/h and with no additional pure oxygen in the inlet air, and the filled squares (■) represent cultivation at a specific growth rate with methanol set at 0.04 1/h and with the inlet air supplemented with pure oxygen to maintain the dissolved oxygen concentration above 20% saturation; in the other two cultivations (● and □), aeration during the methanol production phase was regulated only by increasing the inlet airflow (from 2.5 to 4.0 L/min) and/or agitation speed (up to 1200 rpm). The effects of different specific growth rates with methanol (cultivations ● and □) and oxygen availability (cultivations □ and ■) on cell growth, intracellular EGFP production and extracellular trypsinogen production were compared. Upper graph: cell growth is presented as the logarithm of total biomass with time. Middle graph: intracellular EGFP production is presented as intracellular green fluorescence, as detected by flow cytometry. Bottom graph: extracellular trypsinogen concentration

(Fig. 6, middle graph). This was followed by a rapid decline when the methanol concentration rose to 10 g/L (Fig. 5, top graph). In contrast to results with a low methanol feed rate (μ = 0.018 1/h), where trypsinogen concentration steadily increased over the production time, reaching 64 mg/L at the end of process (in total, 125 mg of trypsinogen was produced), at a specific growth rate μ = 0.035 1/h, stagnation in the extracellular trypsinogen concentration was observed (Fig. 6, bottom graph) as soon as methanol accumulated above a concentration of 3.8 g/L (Fig. 5, top graph). When the methanol concentration in the bioreactor increased to more than 10 g/L, trypsinogen concentration in the medium decreased due to dilution (Fig. 6, bottom graph), reaching a final value of 27 mg/L (total amount of extracellular trypsinogen was 62 mg). Specific trypsinogen production (0.028 ± 0.006 mg/g per h), which was slightly below that measured in the first period of low methanol feeding, dropped to zero when methanol accumulation in bioreactor reached 10 g/L (Table 2). We assume that the activity of trypsin was not affected by methanol accumulation, as it was shown that even 100 g/L methanol does not decrease trypsin activity (Saborowski et al. 2004).

To prevent oxygen limitation and maintain a dissolved oxygen concentration above 20% saturation when a higher exponential feed rate was applied (see dotted line in Fig. 5), cultivation with a specific growth rate of 0.04 1/h and pH 5.9 was repeated, with the aeration gas being supplemented with pure oxygen (Table 2, column 4). Previously, in all processes, aeration during the methanol production phase was regulated only by increasing the inlet airflow and/or agitation speed. Oxygen-enriched aeration gas was able to satisfy the metabolic demands of cells, and only a slight accumulation of methanol was observed at the end of the fed-batch production phase with a high methanol feed rate (Fig. 5). Despite this, a cell-specific growth rate of 0.044 1/h in the bioreactor was not reached until ca 9 h after the start of exponential methanol feeding (Table 2, column 4). The final concentration of biomass reached its highest value of 75 g/L (i.e., ln($x.V$) 5.23 in Fig. 6, upper graph). The fluorescence of intracellular EGFP increased after methanol feeding, indicating the synthesis of recombinant protein, and continued steadily for 12 h; fluorescence then stabilized at a constant level for the rest of the process (Fig. 6, middle graph). Extracellular trypsinogen steadily increased, reaching a maximum of 42 mg/L after 18 h of methanol induction, and then slightly decreased due to dilution, indicating a cessation of production (Fig. 6, bottom graph); this was also indicated by a decrease in specific trypsinogen production, which decreased from 0.032 ± 0.008 mg/g/h to almost zero. Almost 100% viability of cells measured over the first 18 h of the production phase decreased to about 95% in the following 5 h, even though methanol accumulated only slightly, up to 5 g/L, within the last 5 h (Fig. 5, upper graph). In total, 92 mg of trypsinogen was produced under this condition.

Correlation between the intracellular EGFP and extracellular trypsinogen measurements

We wanted to check if there was a correlation between the intracellular and extracellular amounts of the fusion protein EGFP-trypsinogen in the different cultivations. Even though the fusion protein EGFP-trypsinogen was cleaved already inside the cells (Fig. 3), it seemed that the EGFP and trypsinogen fragments were secreted proportionally (Fig. 3b). Therefore, we believe that also the amount of the intracellular EGFP corresponded to the amount of the intracellular trypsinogen. We measured the intracellular fluorescence of EGFP with flow cytometry, and the amount of extracellular trypsinogen by enzymatic assay.

There was no direct correlation between the amount of trypsinogen secreted, and the intracellular EGFP (Fig. 7); the highest intracellular EGFP fluorescence was reached in the cultivation with the lowest specific productivity of trypsinogen, which was at pH 5.9, specific growth rate with methanol set at 0.04 1/h, and no additional oxygen supply. In other processes, the maximum intracellular fluorescence of EGFP was comparable for both pH values and specific growth rates with methanol tested, i.e., independent of the achieved specific productivity of trypsinogen.

In the cultivation with oxygen limitation (empty squares in Figs. 6 and 7), the maximum intracellular EGFP fluorescence was reached after around 16 h of methanol induction (Fig. 6, middle graph), when also the extracellular concentration of trypsinogen reached its maximum (Fig. 6, bottom graph). After this point, the EGFP fluorescence began to decline, and at the end of the cultivation, the fluorescence signal was

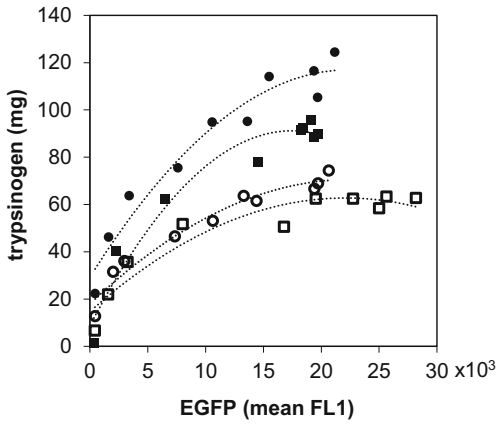

Fig. 7 Trypsinogen production and EGFP-fluorescence over the production phase on methanol in all cultivations. Dotted lines (polynomic curves) indicate the shape of the relationship between intracellular EGFP and trypsinogen, all showing saturation with intracellular EGFP. Cultivation at pH 5.0 (empty circle) and at pH 5.9 (filled circle), at a specific growth rate with methanol set at 0.02 1/h. Cultivation at pH 5.9 at a specific growth rate with methanol set at 0.04 1/h and with no additional pure oxygen in the inlet air (empty square) and with the inlet air supplemented with pure oxygen to maintain the dissolved oxygen concentration above 20% saturation (filled square)

comparable to all other processes. Therefore, assuming that the intracellular EGFP fluorescence refers to the production rate of the fusion protein, it seems that, independent of the cultivation conditions tested, the same "steady state" of production rate was always eventually reached (Fig. 6, middle graph).

Discussion

We have investigated the biotechnological production of recombinant porcine trypsinogen in *Pichia pastoris*. To monitor recombinant protein production as well as to investigate its possible intracellular retention, EGFP was fused to trypsinogen (Fig. 1a). We discuss here the productivity of trypsinogen under specific cultivation conditions, and the suitability of using the EGFP fusion tag for tracking trypsinogen.

EGFP was cleaved from porcine trypsinogen

At both pH 5.0 and 5.9, we observed cleavage of EGFP from the fusion protein EGFP-trypsinogen. The *N*-terminus of the cleaved EGFP fragment began with EAEA, which is the *C*-terminal part of the *S. cerevisiae* α-leader sequence (ending with EKREAEA). This confirms Kex2 cleavage of the α-factor signal sequence between arginine (R) and glutamine (E) (Rockwell et al. 2002), i.e., successful processing of the recombinant protein by its passage into the endoplasmic reticulum. The *N*-terminus of the cleaved trypsinogen part of the fusion protein began with the amino acids tyrosine (Y) and lysine (K), which represent the *C*-terminus of EGFP. Cleavage at the *C*-terminus of EGFP occurred between leucine (L) and tyrosine (Y); this is not a cleavage site for trypsin, which cleaves on the carboxyl side of arginine and lysine (Walsh et al. 1964). The optimum pH for activation of porcine trypsinogen in *Pichia pastoris* was shown to be 8.0 (Shu et al. 2015). No trypsin activity was detected in the medium at pH 6.0 (without treatment with enterokinase), indicating no self-activation of trypsinogen at that pH (Ling et al. 2012). This suggests that autocatalytic activation of trypsinogen with subsequent proteolytic degradation, as one of the possible explanations for the cleavage of the fusion protein (Fig. 1b), did not occur under our cultivation conditions. The cleavage DEL|YK was therefore not performed by trypsin, but rather by extracellular protease(s), cell-bound protease(s), or intracellular protease(s) such as proteinase A, proteinase B, or carboxypeptidases released from lysed cells (Zhang et al. 2007). This phenomenon of non-trypsin cleavage of recombinant porcine trypsinogen, or cleavage of *S. cerevisiae* carboxypeptidase Y produced with *P. pastoris*, was also described in other studies (Shu et al. 2015; Yu et al. 2015). The authors speculated that cleavage might have been initiated by endogenous proteinases (orthologues of proteinase A or B) of *P. pastoris*, released into the cultivation broth. They suggested that the proteinases cleaved the porcine trypsinogen randomly and that the propeptide sequence was excised occasionally, leading ultimately to trypsin formation (Shu et al. 2015). However, the authors did not analyze the cleavage sites. According to our *N*-terminal sequencing results, trypsin was not responsible for the cleavage of EGFP. The degradation of secreted recombinant ovine interferon produced by *P. pastoris* was suggested to be the result of overproduction of proteases, being subsequently mislocalized to the fermentation medium, in combination with leaky membranes caused by cultivation with methanol and cell lysis (Sinha et al. 2005). According to our flow cytometric analysis after PI staining, more than 99% of the cells were unstained, indicating that the cell membranes were not damaged. Therefore, there was no exceptional release of endogenous proteases via cell lysis in our system. At the same time, since we detected cleaved EGFP inside intact cells in all samples analyzed (Fig. 3a), proteolysis of the fusion protein must have started there, probably caused by endogenous proteases. Similarly, proteolytic cleavage of maltose-binding protein (MBP) from a heterologous protein was observed both inside the cells and in the cultivation medium (Li et al. 2010). However, the MBP cleavage inside the cells happened only partially and most of the fusion protein was intact, while we detected only cleaved EGFP inside the cells, indicating that the fusion protein was completely cleaved intracellularly. Cleavage of the secreted fusion protein was dependent on the pH of the cultivation medium. A low pH generally inhibits the activity of proteases (Zhang et al. 2007), which seems to be the case here as well (Fig. 3a); at the higher pH of 5.9, there was a negligible amount of intact fusion protein in the medium, while at pH 5.0, intact fusion protein was detected. Interestingly, the cleavage of MBP persisted even when the heterologous protein was produced in a protease-deficient strain of *P. pastoris* (SMD1163), which excluded the role of proteinase A or B in the cleavage (Li et al. 2010).

To date, very little is known about proteases in *P. pastoris*, especially about those recognizing structural features other than specific amino acid residues (Li et al. 2010). The character of the protease responsible for the cleavage between EGFP and porcine trypsinogen (DEL|YK) remains enigmatic, and we can only assume that it was a mislocalized endogenous protease, eventually in combination with an extracellular protease (Fig. 1b) whose activity was inhibited by low pH. Control experiments such as SDS-PAGE, Western blot, or other immunochemical analysis proved that the integrity of the fusion protein is generally of great importance when using EGFP as a fusion tag. Using these additional analyses, some other authors observed no cleavage of a GFP fusion protein (Surribas et al. 2006, 2007; Tang et al. 2008; Sjöblom et al. 2012), indicating that the cleavage we observed is likely to be product-specific.

Generally speaking, even though there are some concerns about using fluorescent proteins as fusion tags (possible

interference of the tag with protein folding and functionality, increased stress on the cell (Snapp 2005; Siepert et al. 2012), they are irreplaceable when there is a need to monitor proteins in their native, otherwise inaccessible, cellular environments (Snapp 2005) or to measure the dynamics of protein secretion (Sjöblom et al. 2012) in a non-invasive, inexpensive, and labor-saving manner (Broger et al. 2009). Specifically in our case, when producing the fusion protein EGFP-trypsinogen with *P. pastoris*, the purpose of using EGFP to track the potential intracellular accumulation of trypsinogen was prevented by the fact that EGFP was cleaved from the fusion protein. There is a cleavage site at the *C*-terminus of EGFP that may be recognized by some protease(s) in *P. pastoris*, and this fact should be kept in mind when using EGFP as an *N*-terminal fusion tag of recombinant proteins produced by *P. pastoris*. However, it is also possible that the cleavage site was a structural feature that occurred specifically in our fusion protein EGFP-trypsinogen as a consequence of the protein's construction (Li et al. 2010).

Cultivation at pH 5.9 improved the production of trypsinogen by *P. pastoris*

The pH of the cultivation medium (5.0 and 5.9) did not significantly influence cell growth with glycerol ($\mu = 0.2$ 1/h) or methanol ($\mu = 0.02$ 1/h) but had a considerable effect on trypsinogen production. At pH 5.9, the extracellular concentration of trypsinogen over the production phase was 1.7-fold higher than at pH 5.0. Similar results were reported by Viader-Salvado et al. (2013), who observed an insignificant effect of pH 5.0 or 6.0 on growth of *P. pastoris* GS115-derived strain, but ca 3.5-fold higher production of recombinant shrimp trypsinogen in a bioreactor at pH 6.0. In another study (Hyka et al. 2010), it was reported that cultivation at pH 4.0 led to a 5-fold reduction in the expression of recombinant porcine trypsinogen compared to pH 5.0. On the other hand, pH 4.0 contributed to a reduced level of product degradation, while pH 5.0 supported autocatalytic degradation of trypsinogen. Other authors showed that acidic pH values negatively affected the stability of trypsin, causing reversible inactivation, or even irreversible denaturation (Titani et al. 1983; Wu et al. 2008). For example, the optimal pH for the activity of trypsin from the marine crab *Cancer pagurus* was found to be 7.0–9.0 (Saborowski et al. 2004).

Methanol accumulation at a high methanol feeding rate and its elimination by addition of pure oxygen

We analyzed cell growth and recombinant protein production under two different exponential methanol feed rates (i.e., specific growth rates) at pH 5.9 and observed that a higher methanol feed rate (maintaining the specific growth rate at 0.04 1/h) led to oxygen limitation, causing methanol accumulation, reduced cell growth and viability, and affected both the intracellular and extracellular levels of recombinant protein. Methanol accumulated in the bioreactor to a concentration of 3.8 g/L causing accelerated synthesis of recombinant protein but reduced secretion; cell viability was not affected. When the concentration of accumulated methanol exceeded 10 g/L, cell viability started to decrease, the intracellular concentration of EGFP rapidly declined, and specific extracellular production of trypsinogen dropped to zero. Although cell viability was affected by accumulated methanol, with 30 g/L of methanol in the bioreactor, the proportion of PI stained cells (10%) was surprisingly low. However, considering the steadily decreasing cell viability, it could be expected that a higher proportion of PI stained cells would occur with prolonged exposure to excess methanol. It was reported that approximately 30% of *P. pastoris* X-33 cells producing porcine trypsinogen (*AOX1* controlled) were PI-stained if 30 g/L of residual methanol was combined with low pH (4.0); almost 100% of cells were PI-stained if the methanol concentration reached 80 g/L (Hyka et al. 2010). Another work (Gurramkonda et al. 2009) reported that prolonged exposure of cells to methanol had, probably, a greater negative effect than its concentration; the viability of cells grown in the presence of 6 g/L of methanol was initially higher than 90% but declined considerably after 100 h of production phase. In another report, the dead cell fraction was almost 35% after 100 h of cultivation with methanol (Hohenblum et al. 2003). Another work (Ren and Yuan 2005) described a slight inhibitory effect of accumulated methanol (10 g/L) on the growth of *P. pastoris* GS115 cells producing recombinant human serum albumin in a bioreactor, but this significantly depressed recombinant protein production. On the other hand, a strong inhibitory effect of methanol on specific growth rate was reported (Zhang et al. 2000); the authors found that a methanol excess above 3.65 g/L inhibited growth of GS115 strain producing the heavy-chain C fragment of botulinum neurotoxin serotype A at pH 5.0.

Methanol metabolism in *P. pastoris* is generally known to be highly demanding on oxygen supply (Jungo et al. 2007), as confirmed in our work. In our experimental settings, only the use of oxygen-enriched air enabled maintenance of a specific growth rate of 0.04 1/h during the production phase on methanol. However, the addition of pure oxygen, together with large amounts of methanol, would not be desirable in large-scale production due to increased process costs as well as methanol toxicity and flammability. Another approach to resolve technical limitations and avoid economic and security drawbacks would be to use a mixed substrate during the production phase. Glucose was shown to be a successful partial substitute for methanol (Paulova et al. 2012), which led to higher biomass yields and productivities, and lower heat evolution. Another possibility would be to use promoters other than the methanol-inducible alcohol oxidase (*AOX1*)

promoter for recombinant protein expression (Potvin et al. 2012; Ahmad et al. 2014; Yang and Zhang 2017).

Lowered specific growth rate of *P. pastoris* with methanol was beneficial for trypsinogen production

When oxygen-enriched air was used to keep the specific growth rate of cells at 0.04 1/h during the production phase with methanol, the final biomass concentration was 23% higher at the end of cultivation compared to cultivation with a methanol feed designed to maintain μ at 0.02 1/h (both cultivations being performed at pH 5.9). On the other hand, the extracellular trypsinogen concentration reached a steady level after 12 h of methanol feeding at the high specific growth rate, while at the lower specific growth rate, it was increased over the whole production phase. In total, 125 and 92 mg of trypsinogen were produced if the specific growth rate was kept at 0.02 1/h and 0.04 1/h respectively, and oxygen limitation was prevented. As previously reported, the cell-specific growth rate influences the production of recombinant protein (Sinha et al. 2003). The highest production of recombinant ovine interferon was obtained when maintaining a specific growth rate of 0.025 1/h; higher specific growth rates resulted in faster cell metabolism and increased protease production and activity, which led to proteolytic degradation of the product. Having optimized the production of recombinant *Fusarium graminearum* galactose oxidase, it was found that a lower specific growth rate ($\mu = 0.1$ 1/h = 71% μ_{max}) increased the amount of active, correctly folded protein (U/mg) almost 5-fold (Anasontzis et al. 2014).

The highest trypsinogen concentration we achieved was 64 mg trypsinogen per liter at pH 5.9 and a specific growth rate with methanol of 0.018 1/h. Another work reported 480 mg/L of porcine trypsinogen produced with *P. pastoris* after 96 h of methanol induction (Shu et al. 2015). However, until 48 h of induction, the trypsinogen concentration (activity U/L) was approximately 20 times lower, which is comparable to our work. According to Hohenblum et al. (Hohenblum et al. 2003), the amount of secreted human trypsinogen produced by *P. pastoris* was relatively low (below 5 U) in the first 40 h of methanol induction but steeply increased in the following 60 h (up to over 40 U). During continuous cultivation with a mixed substrate (methanol with glucose) at a dilution rate of 0.03 1/h, over 200 mg of non-tagged porcine trypsinogen per liter was achieved (Paulova et al. 2012).

Conclusions

The production of a fusion protein of EGFP and porcine trypsinogen and the physiology of *P. pastoris* strain (e.g., membrane defects indicated by PI staining) were analyzed at two different pH values (5.0 and 5.9) and two different specific growth rates with methanol (0.02 1/h and 0.04 1/h). The pH of the culture medium affected neither biomass growth nor cell viability, whereas the production of the fusion protein was considerably affected by both pH and specific growth rate with methanol. As no severe impairments in cell growth or integrity of the cell membrane were detected, we concluded that trypsinogen did neither accumulate intracellularly to a harmful extent nor was it proteolytically activated to trypsin. Cleavage of the EGFP-trypsinogen fusion protein was observed, probably caused by cellular proteases. In our opinion, such information is useful for further identification and characterization of proteolytic enzymes in *P. pastoris*, the description of which may be used to improve the yeast's application as a host for production of secreted proteins. Furthermore, these results show the importance of additional analyses (Western blot, SDS-PAGE) to avoid misinterpretation of tracking and quantifying with online-monitoring proteins using fluorescent tags. Using a combination of a routine analysis of the secreted protein (in the medium outside the cell) with assessment of the intracellular accumulation of this product and cell viability, it was found that intracellular accumulation continuously increased and reached saturation level independent of cultivation conditions tested (pH, specific growth rate with methanol). This observation brings new insights into the kinetics of recombinant protein production in *P. pastoris*.

Acknowledgements This work was supported by the project MSM6046137305 and built on research performed within the Czech-Swiss project with the participation of Lonza AG and Lonza Biotec s.r.o. E!3415 Optytech, 1P05OE189 of Ministry of Education, Youth and Sports of the Czech Republic and the KTI-Project 7403.3;3 LSPP-LS (https://www.aramis.admin.ch/Grunddaten/?ProjectID=21894). The authors thank Zdeněk Voburka for the *N*-terminal sequencing analysis, Iwo Zamora for help with data analysis, Katrin Hecht for critical reading of the manuscript, and John Brooker and Maggi Lussi Bell for English proofreading.

References

Ahmad M, Hirz M, Pichler H, Schwab H (2014) Protein expression in *Pichia pastoris*: recent achievements and perspectives for heterologous protein production. Appl Microbiol Biotechnol 98:5301–5317. https://doi.org/10.1007/s00253-014-5732-5

Anasontzis GE, Pena MS, Spadiut O et al (2014) Effects of temperature and glycerol and methanol-feeding profiles on the production of recombinant galactose oxidase in *Pichia pastoris*. Biotechnol Prog 30:728–735. https://doi.org/10.1002/btpr.1878

Broger T, Odermatt RP, Ledergerber P, Sonnleitner B (2009) Exploiting fluorescent reporter molecules for process analytical technology (PAT). Chim Int J Chem 63:171–173. https://doi.org/10.2533/chimia.2009.171

Guerrero-Olazaran M, Escamilla-Trevino LL, Castillo-Galvan M et al (2009) Recombinant shrimp (*Litopenaeus vannamei*) trypsinogen

production in *Pichia pastoris*. Biotechnol Prog 25:1310–1316. https://doi.org/10.1002/btpr.197

Gurramkonda C, Adnan A, Gabel T et al (2009) Simple high-cell density fed-batch technique for high-level recombinant protein production with *Pichia pastoris*: application to intracellular production of hepatitis B surface antigen. Microb Cell Factories 8:8. https://doi.org/10.1186/1475-2859-8-13

Hanquier J, Sorlet Y, Desplancq D, Baroche L, Ebtinger M, Lefevre JF, Pattus F, Hershberger CL, Vertes AA (2003) A single mutation in the activation site of bovine trypsinogen enhances its accumulation in the fermentation broth of the yeast *Pichia pastoris*. Appl Environ Microbiol 69:1108–1113

Hohenblum H, Borth N, Mattanovich D (2003) Assessing viability and cell-associated product of recombinant protein producing *Pichia pastoris* with flow cytometry. J Biotechnol 102:281–290

Hyka P, Zullig T, Ruth C, Looser V, Meier C, Klein J, Melzoch K, Meyer HP, Glieder A, Kovar K (2010) Combined use of fluorescent dyes and flow cytometry to quantify the physiological state of *Pichia pastoris* during the production of heterologous proteins in high-cell-density fed-batch cultures. Appl Environ Microbiol 76:4486–4496. https://doi.org/10.1128/AEM.02475-09

Jungo C, Marison I, von Stockar U (2007) Mixed feeds of glycerol and methanol can improve the performance of *Pichia pastoris* cultures: a quantitative study based on concentration gradients in transient continuous cultures. J Biotechnol 128:824–837. https://doi.org/10.1016/j.jbiotec.2006.12.024

Juturu V, Wu JC (2018) Heterologous protein expression in *Pichia pastoris*: latest research progress and applications. ChemBioChem 19:7–21

Kunitz M, Northrop JH (1934) Inactivation of crystalline trypsin. J Gen Physiol 17:591–615

Li Z, Leung W, Yon A, Nguyen J, Perez VC, Vu J, Giang W, Luong LT, Phan T, Salazar KA, Gomez SR, Au C, Xiang F, Thomas DW, Franz AH, Lin-Cereghino J, Lin-Cereghino GP (2010) Secretion and proteolysis of heterologous proteins fused to the *Escherichia coli* maltose binding protein in *Pichia pastoris*. Protein Expr Purif 72:113–124. https://doi.org/10.1016/j.pep.2010.03.004

Ling Z, Kang Z, Liu Y, Liu S, Chen J, du G (2014) Improvement of catalytic efficiency and thermostability of recombinant *Streptomyces griseus* trypsin by introducing artificial peptide. World J Microbiol Biotechnol 30:1819–1827. https://doi.org/10.1007/s11274-014-1608-1

Ling ZM, Ma TB, Li JH, du G, Kang Z, Chen J (2012) Functional expression of trypsin from *Streptomyces griseus* by *Pichia pastoris*. J Ind Microbiol Biotechnol 39:1651–1662. https://doi.org/10.1007/s10295-012-1172-3

Looser V, Bruhlmann B, Bumbak F, Stenger C, Costa M, Camattari A, Fotiadis D, Kovar K (2015) Cultivation strategies to enhance productivity of *Pichia pastoris*: a review. Biotechnol Adv 33:1177–1193. https://doi.org/10.1016/j.biotechadv.2015.05.008

Macouzet M, Simpson BK, Lee BH (2005) Expression of a cold-adapted fish trypsin in *Pichia pastoris*. FEMS Yeast Res 5:851–857. https://doi.org/10.1016/j.femsyr.2005.02.007

Paulova L, Hyka P, Branska B et al (2012) Use of a mixture of glucose and methanol as substrates for the production of recombinant trypsinogen in continuous cultures with *Pichia pastoris* Mut+. J Biotechnol 157:180–188. https://doi.org/10.1016/j.jbiotec.2011.10.010

Potgieter TI, Kersey SD, Mallem MR, Nylen AC, d'Anjou M (2010) Antibody expression kinetics in glycoengineered *Pichia pastoris*. Biotechnol Bioeng 106:918–927. https://doi.org/10.1002/bit.22756

Potvin G, Ahmad A, Zhang ZS (2012) Bioprocess engineering aspects of heterologous protein production in *Pichia pastoris*: a review. Biochem Eng J 64:91–105. https://doi.org/10.1016/j.bej.2010.07.017

Ren HT, Yuan JQ (2005) Model-based specific growth rate control for *Pichia pastoris* to improve recombinant protein production. J Chem Technol Biotechnol 80:1268–1272. https://doi.org/10.1002/jctb.1321

Rockwell NC, Krysan DJ, Komiyama T, Fuller RS (2002) Precursor processing by Kex2/furin proteases. Chem Rev 102:4525–4548. https://doi.org/10.1021/cr010168i

Saborowski R, Sahling G, Navarette Del Toro MA et al (2004) Stability and effects of organic solvents on endopeptidases from the gastric fluid of the marine crab *Cancer pagurus*. J Mol Catal B Enzym 30:109–118. https://doi.org/10.1016/j.molcatb.2004.04.002

Shu M, Shen W, Wang XJ, Wang F, Ma L, Zhai C (2015) Expression, activation and characterization of porcine trypsin in *Pichia pastoris* GS115. Protein Expr Purif 114:149–155. https://doi.org/10.1016/j.pep.2015.06.014

Siepert EM, Gartz E, Tur MK, Delbrück H, Barth S, Büchs J (2012) Short-chain fluorescent tryptophan tags for on-line detection of functional recombinant proteins. BMC Biotechnol 12:65. https://doi.org/10.1186/1472-6750-12-65

Sinha J, Plantz BA, Inan M, Meagher MM (2005) Causes of proteolytic degradation of secreted recombinant proteins produced in methylotrophic yeast *Pichia pastoris*: case study with recombinant ovine interferon-tau. Biotechnol Bioeng 89:102–112. https://doi.org/10.1002/bit.20318

Sinha J, Plantz BA, Zhang W, Gouthro M, Schlegel V, Liu CP, Meagher MM (2003) Improved production of recombinant ovine interferon-tau by mut(+) strain of *Pichia pastoris* using an optimized methanol feed profile. Biotechnol Prog 19:794–802. https://doi.org/10.1021/bp025744q

Sjöblom M, Lindberg L, Holgersson J, Rova U (2012) Secretion and expression dynamics of a GFP-tagged mucin-type fusion protein in high cell density *Pichia pastoris* bioreactor cultivations. Adv Biosci Biotechnol 3:238–248. https://doi.org/10.4236/abb.2012.33033

Snapp E (2005) Design and Use of Fluorescent Fusion Proteins in Cell Biology. Curr Protoc Cell Biol. https://doi.org/10.1002/0471143030.cb2104s27

Surribas A, Resina D, Ferrer P, Valero F (2007) Rivoflavin may interfere with on-line monitoring of secreted green fluorescence protein fusion proteins in *Pichia pastoris*. Microb Cell Factories 6:15. https://doi.org/10.1186/1475-2859-6-15

Surribas A, Resina D, Ferrer P, Valero F (2006) Limitations using GFP as a protein expression reporter in *Pichia pastoris*. Microb Cell Factories 5:P56. https://doi.org/10.1186/1475-2859-5-s1-p56

Tang JB, Zhu P, Yang HM, Sun LM, Song SL, Ji AG (2008) Expression and secretion of recombinant ZZ-EGFP fusion protein by the methylotrophic yeast *Pichia pastoris*. Biotechnol Lett 30:1409–1414. https://doi.org/10.1007/s10529-008-9714-5

Titani K, Sasagawa T, Woodbury RG, Ericsson LH, Dorsam H, Kraemer M, Neurath H, Zwilling R (1983) Amino acid sequence of crayfish (*Astacus fluviatilis*) trypsin If. Biochemistry 22:1459–1465. https://doi.org/10.1021/bi00275a021

Viader-Salvado JM, Fuentes-Garibay JA, Castillo-Galvan M et al (2013) Shrimp (*Litopenaeus vannamei*) trypsinogen production in *Pichia pastoris* bioreactor cultures. Biotechnol Prog 29:11–16. https://doi.org/10.1002/btpr.1646

Walsh KA, Kauffman DL, Kumar KSVS, Neurath H (1964) On the structure and function of bovine trypsinogen and trypsin. Proc Natl Acad Sci U S A 51:301–308

Whiting DR, Guariguata L, Weil C, Shaw J (2011) IDF diabetes atlas: global estimates of the prevalence of diabetes for 2011 and 2030. Diabetes Res Clin Pract 94:311–321. https://doi.org/10.1016/j.diabres.2011.10.029

Wu Z, Jiang G, Xiang P, Xu H (2008) Anionic trypsin from North Pacific krill (*Euphausia pacifica*): purification and characterization. Int J Pept Res Ther 14:113–120. https://doi.org/10.1007/s10989-007-9119-7

Yamada Y, Maeda K, Mikata K (1994) The phylogenetic relationships of the hat-shaped ascospore-forming, nitrate-assimilating *Pichia* species, formerly classified in the genus *Hansenula* Sydow et Sydow, based on the partial sequences of 18S and 26S ribosomal RNAs (Saccharomycetaceae): the proposals of three new genera, *Ogataea*, *Kuraishia*, and *Nakazawaea*. Biosci Biotechnol Biochem 58:1245–1257. https://doi.org/10.1271/bbb.58.1245

Yamada Y, Matsuda M, Maeda K, Mikata K (1995) The phylogenetic relationships of methanol-assimilating yeasts based on the partial sequences of 18S and 26S ribosomal RNAs: the proposal of *Komagataella* gen. nov. (Saccharomycetaceae). Biosci Biotechnol Biochem 59:439–444. https://doi.org/10.1271/bbb.59.439

Yang Z, Zhang Z (2017) Engineering strategies for enhanced production of protein and bio-products in *Pichia pastoris*: a review. Biotechnol Adv 36(1):182–195

Yu XH, Zhai C, Zhong X, Tang W, Wang X, Yang H, Chen W, Ma L (2015) High-level expression and characterization of carboxypeptidase Y from *Saccharomyces cerevisiae* in *Pichia pastoris* GS115. Biotechnol Lett 37:161–167. https://doi.org/10.1007/s10529-014-1667-2

Zahrl RJ, Peña DA, Mattanovich D, Gasser B (2017) Systems biotechnology for protein production in *Pichia pastoris*. FEMS Yeast Res 17. https://doi.org/10.1093/femsyr/fox068

Zhang WH, Bevins MA, Plantz BA, Smith LA, Meagher MM (2000) Modeling *Pichia pastoris* growth on methanol and optimizing the production of a recombinant protein, the heavy-chain fragment C of botulinum neurotoxin, serotype A. Biotechnol Bioeng 70:1–8. https://doi.org/10.1002/1097-0290(20001005)70:1<1::aid-bit1>3.0.co;2-y

Zhang Y, Huang H, Yao X, du G, Chen J, Kang Z (2018) High-yield secretory production of stable, active trypsin through engineering of the N-terminal peptide and self-degradation sites in *Pichia pastoris*. Bioresour Technol 247:81–87. https://doi.org/10.1016/j.biortech.2017.08.006

Zhang Y, Liu R, Wu X (2007) The proteolytic systems and heterologous proteins degradation in the methylotrophic yeast *Pichia pastoris*. Ann Microbiol 57:553–560